



HAL
open science

Modelling the second wave of COVID-19 infections in France and Italy via a Stochastic SEIR model

Davide Faranda, Tommaso Alberti

► **To cite this version:**

Davide Faranda, Tommaso Alberti. Modelling the second wave of COVID-19 infections in France and Italy via a Stochastic SEIR model. *Chaos: An Interdisciplinary Journal of Nonlinear Science*, 2020, 30, pp.111101. 10.1063/5.0015943 . hal-02668318v3

HAL Id: hal-02668318

<https://hal.science/hal-02668318v3>

Submitted on 8 Oct 2020

HAL is a multi-disciplinary open access archive for the deposit and dissemination of scientific research documents, whether they are published or not. The documents may come from teaching and research institutions in France or abroad, or from public or private research centers.

L'archive ouverte pluridisciplinaire **HAL**, est destinée au dépôt et à la diffusion de documents scientifiques de niveau recherche, publiés ou non, émanant des établissements d'enseignement et de recherche français ou étrangers, des laboratoires publics ou privés.

1 **Modelling the second wave of COVID-19 infections in France and Italy via a**
2 **Stochastic SEIR model**

3 Davide Faranda^{1,2,3, a)} and Tommaso Alberti⁴

4 ¹⁾*Laboratoire des Sciences du Climat et de l'Environnement,*
5 *CEA Saclay l'Orme des Merisiers, UMR 8212 CEA-CNRS-UVSQ,*
6 *Université Paris-Saclay & IPSL, 91191, Gif-sur-Yvette, France*

7 ²⁾*London Mathematical Laboratory, 8 Margravine Gardens, London, W6 8RH,*
8 *UK*

9 ³⁾*LMD/IPSL, Ecole Normale Supérieure, PSL research University, 75005, Paris,*
10 *France*

11 ⁴⁾*INAF - Istituto di Astrofisica e Planetologia Spaziali, via del Fosso del Cavaliere 100,*
12 *00133 Roma, Italy*

13 (Dated: 7 October 2020)

14 COVID-19 has forced quarantine measures in several countries across the world. These
15 measures have proven to be effective in significantly reducing the prevalence of the virus.
16 To date, no effective treatment or vaccine is available. In the effort of preserving both
17 public health as well as the economical and social textures, France and Italy governments
18 have partially released lockdown measures. Here we extrapolate the long-term behav-
19 ior of the epidemics in both countries using a Susceptible-Exposed-Infected-Recovered
20 (SEIR) model where parameters are stochastically perturbed with a log-normal distribu-
21 tion to handle the uncertainty in the estimates of COVID-19 prevalence and to simulate
22 the presence of super-spreaders. Our results suggest that uncertainties in both parameters
23 and initial conditions rapidly propagate in the model and can result in different outcomes
24 of the epidemics leading or not to a second wave of infections. Furthermore, the presence
25 of super-spreaders adds instability to the dynamics, making the control of the epidemics
26 more difficult. Using actual knowledge, asymptotic estimates of COVID-19 prevalence
27 can fluctuate of order of ten millions units in both countries.

^{a)}Correspondence to davide.faranda@lscce.ipsl.fr

28 I. LEAD PARAGRAPH

29 **COVID-19 pandemic poses serious threats to public health as well as economic and so-**
30 **cial stability of many countries. A real time extrapolation of the evolution of COVID-19**
31 **epidemics is challenging both for the nonlinearities undermining the dynamics and the ig-**
32 **norance of the initial conditions, i.e., the number of actual infected individuals. Here we**
33 **focus on France and Italy, which have partially released initial lockdown measures. The**
34 **goal is to explore sensitivity of COVID-19 epidemic evolution to the release of lockdown**
35 **measures using dynamical (Susceptible-Exposed-Infected-Recovered) stochastic models. We**
36 **show that the large uncertainties arising from both poor data quality and inadequate estima-**
37 **tions of model parameters (incubation, infection and recovery rates) propagate to long term**
38 **extrapolations of infections counts. Nonetheless, distinct scenarios can be clearly identified,**
39 **showing either a second wave or a quasi-linear increase of total infections.**

40 II. INTRODUCTION

41 SARS-CoV-2 is a zoonotic virus of the coronavirus family¹ emerged in Wuhan (China) at the
42 end of 2019² and rapidly propagated across the world until it has been declared a pandemic by
43 the World Health Organization on March 11, 2020³. SARS-CoV-2 virus provokes an infectious
44 disease known as COVID-19 that has an incredibly large spectrum of symptoms or none depending
45 on the age, health status and the immune defenses of each individuals⁴. SARS-CoV-2 causes
46 potentially life-threatening form of pneumonia and/or cardiac injuries in a non-negligible patients
47 fraction^{5,6}.

48 To date, no treatment of vaccine is available for COVID-19⁷. Efforts to contain the virus and
49 to not overwhelm intensive care facilities are based on quarantine measures which have proven
50 very effective in several countries⁸⁻¹⁰. These predictions were based on statistical and epidemi-
51 ological models that, despite their simplicity, well captured the growths of the epidemics¹¹⁻¹³.
52 Despite this, lockdown measures entail enormous economical, social and psychological costs. Re-
53 cent estimates of the International Monetary Fund recently announced a global recession that will
54 drag global GDP lower by 3% in 2020, although continuously developing and changing as well
55 as significantly depending country-by-country¹⁴. More than 20 million people have lost their job
56 in United States¹⁵ and a large percentage of Italians have developed psychological disturbances

57 such as insomnia or anxiety due to the strict lockdown measures¹⁶. Those measures have been
58 taken on the basis of epidemics models, which are fitted on the available data¹⁷. In Italy, initial
59 lockdown measures started on February 23rd for 11 municipalities in both Lombardia and Veneto
60 which were identified as the two main Italian clusters. After the initial spread of the epidemics
61 into different regions all Italian territory was placed into a quarantine on March 9th, with total
62 lockdown measures including all commercial activities (apart supermarkets and pharmacies), non-
63 essential businesses and industries, and severe restrictions to transports and movements of people
64 at regional, national, and extra-national levels¹⁸. People were asked to stay at home or near for
65 sporting activities and dog hygiene (within 200 m from home), to reduce as much as possible their
66 movements (only for food shopping and care reasons), and smart-working was especially encour-
67 aged in both public and private administrations and companies. At the early stages of epidemics
68 intensive cares were almost saturated with a peak of 4000 people on April 3rd and a peak of
69 hospitalisations of 30000 on April 4th, significantly reducing after these dates, reaching 1500
70 and 17000, respectively, at the beginning of phase 2 on May 4th, and 750 and 1000 on May 18th
71 when lockdown measures on commercial activities were relaxed. These numbers, continuously
72 declining during the next days and weeks, confirmed the benefit of lockdown measures¹⁹.

73 Alarmed by the exponential growth of new infections and the saturation of the intensive care beds,
74 also France introduced strict lockdown measures on March 17th²⁰. The French government re-
75 stricted travels to food shopping, care and work when teleworking was not possible, outings near
76 home for individual sporting activity and/or dog hygiene, and it imposed the closure of the Schen-
77 gen area borders as well as the postponement of the second round of municipal elections. The
78 number of patients in intensive care, like the number of hospitalisations overall peaked in early
79 April and then started to decline, showing the benefits of lockdown measures. On Monday, May
80 11th, France began a gradual easing of COVID-19 lockdown measures²¹. Trips of up to 100 kilo-
81 metres from home are allowed without justification, as will gatherings of up to 10 people. Longer
82 trips will still be allowed only for work or for compelling family reasons, as justified by a signed
83 form. Guiding the government's plans for easing the lockdown is the division of the country into
84 two zones, green and red, based on health indicators. Paris region (Ile de France), with about 12
85 millions inhabitants is flagged, to date, as an orange zone.

86 In both countries, the release of lockdown measures has been authorised by authorities after
87 consulting scientific committees which were monitoring the behavior of the curve of infections
88 using COVID-19 data. Those data are provided daily, following a request of the WHO. To date,

89 the WHO guidelines require countries to report, at each day t , the total number of infected patients
90 $I(t)$ as well as the number of deaths $D(t)$. Large uncertainties have been documented in the count
91 of $I(t)$ ²². Whereas in the early stage of the epidemic several countries tested asymptomatic indi-
92 viduals to track back the infection chain, recent policies to estimate $I(t)$ have changed. Most of
93 the western countries have previously tested only patients displaying severe SARS-CoV-2 symp-
94 toms²³. In an effort of tracking all the chain of infections, Italy and France are now testing all
95 individuals displaying COVID-19 symptoms and those who had strict contacts with infected indi-
96 viduals. The importance of tracking asymptomatic patients has been proven in a recent study²⁴.
97 The authors have estimated that an enormous part of total infections were undocumented (80% to
98 90%) and that those undetected infections were the source for 79% of documented cases in China.
99 Tracking strategies have proven effective in supporting actions to reduce the rate of new infections,
100 without the need of lockdown measures, as in South Korea²⁵.

101 The goal of this paper is to explore possible future epidemics scenarios of the long term be-
102 havior of the COVID-19 epidemic²⁶ but taking into account the role of uncertainties in both
103 the parameters value and the infection counts to investigate different outcomes of the epidemics
104 leading or not to a second wave of infections. To this purpose we use a stochastic Susceptible-
105 Exposed-Infected-Recovered (SEIR) model²⁷ which consists in a set of ordinary differential equa-
106 tions where control parameters are time-dependent and modelled via a stochastic process. This
107 allows to mimic the dependence on control parameters on some additional/external factors as
108 super-spreaders²⁸ and the enforcing/relaxing of confinement measures²⁷. As for the classical SEIR
109 models²⁹ the population is divided into four compartmental groups, i.e., Susceptible, Exposed, In-
110 fected, and Recovered individuals. The stochastic SEIR model shows that long-term extrapolation
111 is sensitive to both the initial conditions and the value of control parameters²⁷, with asymptotic
112 estimates fluctuating on the order of ten millions units in both countries, leading or not a second
113 wave of infections. This sensitivity arising from both poor data quality and inadequate estimations
114 of model parameters has been also recently investigated by means of a statistical model based on a
115 generalized logistic distribution^{30,31}. The paper is organised as follows: in Section III we discuss
116 the various sources of data for COVID-19 and their shortcomings, and then we discuss in detail
117 the SEIR model and its statistical modelling. In Section IV we discuss the results focusing on the
118 statistical sensitivity of the modelling, and apply it to data from France and Italy. We finish, in
119 Section V, with some remarks and point out some limitations of our study.

120 III. DATA AND MODELLING

121 A. Data

122 This paper relies on data stored into the Visual Dashboard repository of the Johns Hopkins Uni-
123 versity Center for Systems Science and Engineering (JHU CSSE) supported by ESRI Living Atlas
124 Team and the Johns Hopkins University Applied Physics Lab (JHU APL). Data can be freely
125 accessed and downloaded at <https://systems.jhu.edu/research/public-health/ncov/>,
126 and refers to the confirmed cases by means of a laboratory test³. Nevertheless there are some
127 inconsistencies between countries due to different protocols in testing patients (suspected symp-
128 toms, tracing-back procedures, wide range tests)^{32,33}, as well as, to local management of health
129 infrastructures and institutions. As an example due to the regional-level system of Italian health-
130 care data are collected at a regional level and then reported to the National level via the Protezione
131 Civile transferring them to WHO. These processes could be affected by some inconsistencies and
132 delays³⁴, especially during the most critical phase of the epidemic diffusion that could introduce
133 errors and biases into the daily data. These incongruities mostly affected the period between Febru-
134 ary 23rd and March 10th, particularly regarding the counts of deaths due to a protocol change from
135 the Italian Ministry of Health³⁵. A similar situation occurs in France where the initial testing strat-
136 egy was based only on detecting those individuals experiencing severe COVID19 symptoms³⁶.
137 In the post lockdown phase, France has extended its testing capacity to asymptomatic individuals
138 who have been in contact with infected patients³⁷.

139 B. A Stochastic epidemiological Susceptible-Exposed-Infected-Recovered model

140 One of the most used epidemiological models is the so-called Susceptible-Exposed-Infected-
141 Recovered (SEIR) model belonging to the class of compartmental models²⁹. It assumes that the
142 total population N can be divided into four classes of individuals that are susceptible S , exposed
143 E , infected I , and recovered or dead R (assumed to be not susceptible to reinfection). The model
144 is based on the following assumptions:

- 145 1. the total population does not vary in time, e.g., $dN/dt = dS/dt + dE/dt + dI/dt + dR/dt =$
146 $0, \forall t \geq 0$;
- 147 2. susceptible individuals become infected that then can only recover or die, e.g., $S \rightarrow I \rightarrow R$;

148 3. exposed individuals E encountered an infected person but are not yet themselves infectious;

149 4. recovered or died individuals R are forever immune. Although the longevity of the antibody

150 response is still unknown, it is known that antibodies to other coronaviruses wane over time

151 typically after 52 weeks from the onset of symptoms³⁸. Concerning SARS-CoV-2 it has

152 been shown that antibody levels may remain over the course of almost 2-3 months³⁹. Never-

153 theless, not only antibodies are important for investigating immunity but also other immune

154 cells named T cells play a crucial role for long-term immunity^{40,41}. Recently Kissler et al.⁴²

155 found that the duration of protective immunity may last 6 to 12 months. Our assumption

156 seems therefore justified at least to study the dynamics of a second wave. We remark also

157 that the basic SEIR model does not distinguish between immune and deaths and it cannot

158 therefore be used to estimate the number of deceased people from COVID-19.

159 Thus, the model reads as

$$160 \quad \frac{dS}{dt} = -\lambda S(t)I(t), \quad (1)$$

$$161 \quad \frac{dE}{dt} = \lambda S(t)I(t) - \alpha E(t), \quad (2)$$

$$162 \quad \frac{dI}{dt} = \alpha E(t) - \gamma I(t), \quad (3)$$

$$163 \quad \frac{dR}{dt} = \gamma I(t), \quad (4)$$

164 where $\gamma > 0$ is the recovery/death rate, $\lambda = \lambda_0/S(0) > 0$ is the infection rate rescaled by the initial

165 number of susceptible individuals $S(0)$, and α is the inverse of the incubation period. Its discrete

166 version can be simply obtained via an Euler Scheme as

$$167 \quad S(t+1) = S(t) - \lambda S(t)I(t), \quad (5)$$

$$168 \quad E(t+1) = (1 - \alpha)E(t) + \lambda S(t)I(t), \quad (6)$$

$$169 \quad I(t+1) = (1 - \gamma)I(t) + \alpha E(t), \quad (7)$$

$$170 \quad R(t+1) = R(t) + \gamma I(t). \quad (8)$$

171 in which we fixed $dt = 1$ day that is the time resolution of COVID-19 counts. By means of γ

172 and λ_0 the model also allows to derived the so-called R_0 parameter, e.g., $R_0 = \lambda_0/\gamma$, representing

173 the average reproduction number of the virus. It is related to the number of cases that can poten-

174 tially (on average) be caused from an infected individual during its infectious period ($\tau_{inf} = \gamma^{-1}$).

175 Early estimates in Wuhan⁴³ on January 2020 reported $R_0 = 2.68_{2.47}^{2.86}$ which lead to $\gamma = \gamma_0 = 0.37$
176 fixing $\lambda \simeq 1$ as in⁴⁴ and a 95% confidence level range for the incubation period between 2 and
177 11 days⁴⁵. Here we set $\alpha = \alpha_0 = 0.27$ (corresponding to an incubation period between 3 and 4
178 days). This value has been extracted as median period by⁴⁵. However, the R_0 parameter as well
179 as models parameters λ , γ , and α can vary in time during the epidemics due to different factors
180 as the possible presence of the so-called super-spreaders²⁸, intrinsic changes of the SARS-CoV-2
181 features, lockdown measures, asymptomatic individuals who are not tracked out, counting proce-
182 dures and protocols, and so on⁴⁶. The fact that all the time-scales considered for the parameters
183 are larger than one day also justifies the use of the discrete version of the model in Eqs. 5-8.

184 To deal with uncertainties in long-term extrapolations and with the time-dependency of control
185 parameters a stochastic approach could provide new insights in modeling epidemics⁴⁷⁻⁴⁹, espe-
186 cially when epidemics show a wide range of spatial and temporal variability⁵⁰⁻⁵². However,
187 instead of investigating how to get a realistic behavior by stochastically perturbing control pa-
188 rameters, here we investigate how uncertainties into the final counts $C(t)$ are controlled by model
189 parameters²⁷. Thus, we use a stochastic version of the SEIR model in which the set of con-
190 trol parameters $\kappa \in \{\alpha, \gamma, \lambda\}$ are extracted at each timestep from random distributions. In the
191 ODE model (Eqs 1-4) the introduction of stochastic terms corresponds to replacing $\{\alpha, \gamma, \lambda\}$ with
192 $\{\alpha(t), \gamma(t), \lambda(t)\}$ and adding three more differential equations of the type:

$$193 \quad \frac{d\kappa}{dt} = -\kappa(t) + \kappa_0 + \zeta_{\kappa}\xi(t), \quad (9)$$

194 where $\kappa_0 \in \{\alpha_0, \gamma_0, \lambda_0\}$, $\xi(t)$ is a random number extracted from a normal distribution for α, γ
195 and from a log-normal distribution for λ (see below). The stochastic model therefore reads as:

$$196 \quad dS = -\lambda(t)S(t)I(t)dt, \quad (10)$$

$$197 \quad dE = [\lambda(t)S(t)I(t) - \alpha(t)E(t)]dt, \quad (11)$$

$$198 \quad dI = [\alpha(t)E(t) - \gamma I(t)]dt, \quad (12)$$

$$199 \quad dR = \gamma(t)I(t)dt, \quad (13)$$

$$200 \quad d\lambda = \lambda_0 dt + \zeta_{\lambda} dW(t), \quad (14)$$

$$201 \quad d\alpha = \alpha_0 dt + \zeta_{\alpha} dW(t), \quad (15)$$

$$202 \quad d\gamma = \gamma_0 dt + \zeta_{\gamma} dW(t), \quad (16)$$

203 where $dW(t) = \xi(t)dt$ is the differential form of the Brownian motion. In order to test the
 204 stability of our model integrated with the Euler scheme (see MATLAB code in the Appendix), we
 205 perform 30 realisations of Eqs 10-16 with the aforementioned parameters and initial conditions
 206 $S(1) = 67 \cdot 10^6$ (French population), $I(1) = 1$, $E(1) = R(1) = 0$. We vary dt in the range $0.1 <$
 207 $dt < 2$. Results are displayed in Figure 1 in terms of daily infections $I(t)$. They show the typical
 208 bell-shaped curve of an epidemic wave. We get high stability of the integration when $dt \leq 1$. For
 209 larger values, the epidemic peak is first delayed ($dt = 1.5$) and the model diverges (not shown)
 210 for $dt = 2$. In the following, we decide to stick to $dt = 1$, which will be convenient to compare
 211 our results with those released by the national health agencies as in both the countries data are
 212 provided on a daily basis.

213 With the choice of $dt = 1$ day, one trivially gets that Eq. 9 is equivalent to sampling $\alpha(t) \in$
 214 $\mathcal{N}(\alpha_0, \zeta_\alpha^2; t)$, $\gamma(t) \in \mathcal{N}(\gamma_0, \zeta_\gamma^2; t)$ and

$$215 \log(\lambda(t)) \in \mathcal{N}(\log(\lambda_0 - \sigma^2/2), \sigma; t). \tag{17}$$

216 In this way we can introduce instantaneous daily discrete jumps (e.g., take into account daily
 217 uncertainties) in the control parameters to properly model detection errors on infection counts,
 218 appropriately described through a discrete process⁵³ rather than a continuous one⁵⁴. For α and γ
 219 we follow²⁷ and allow for Gaussian fluctuations of the parameters, with intensity $\zeta_\alpha = 0.2\alpha_0$ and
 220 $\zeta_\gamma = 0.2\gamma_0$. These fluctuations simulate the range of uncertainties obtained in previous studies for
 221 the incubation time and the recovery time and discussed in²⁷. With respect to²⁷, we model the
 222 infection rate $\lambda(t)$ using a log-normal distribution⁵⁵ to take into account the possible presence of
 223 super-spreaders, namely individuals who can infect quickly a large number of susceptible people
 224 by having several strict social interactions⁵⁶. Super-spreaders can be modelled by introducing
 225 heavy right tails for the distribution of λ . The location and the scale parameters chosen in Eq. 17
 226 ensures that the mean of the distribution does not change, while σ is modified to explore super-
 227 spreaders influence. In the following, we will only consider three cases: i) $\sigma = 0.2$ for which the
 228 log-normal distribution tends to be symmetric and the fluctuations of λ are quasi-Gaussian around
 229 λ_0 , ii) $\sigma = 0.4$ which models the effect of some possible super-spreaders and $\sigma = 0.6$ where
 230 several super-spreaders may be active at the same time.

231 IV. RESULTS

232 A. Model validation: first wave

233 We begin this section by validating the SEIR stochastic model on the first wave of infections.
234 We have therefore to chose the initial conditions, and then introduce the lockdown measures in the
235 parameters.

236 a. France

237 In France, the first documented case of COVID-19 infections goes back to December 27th, 2019.
238 Doctors at a hospital in the northern suburbs of Paris retested samples from patients between De-
239 cember 2nd, 2019, and January 16th, 2020. Of the 14 patient samples retested, one sample, from
240 a 42-year-old man came back positive⁵⁷. As initial condition for the SEIR model, we therefore set
241 $I(t = 1) = 1$ and $t = 1$ corresponds to December 27th, 2019. We then use $R_0 = 2.68_{2.47}^{2.86}$ which
242 lead to $\gamma = 0.37$ fixing $\lambda_0 \simeq 1$. Strict lockdown measures are introduced at $t = 80$ (i.e., March
243 17th, 2020). First wave modelling results are shown in Figure 2. Figure 2a) shows the modelled
244 value of R_0 . During confinement, we reduce the value of λ_0 by a factor 1/4. We base this new
245 infection rate on the mobility data for France during confinement, which have shown a drop by
246 $\sim 75\%$ according to the INSERM report #11⁵⁸. The resulting confinement $R_0 \simeq 0.75$, with an
247 error in the range of values compatible with that published by the Pasteur Institute⁵⁹, for all values
248 of σ of the log-normal distribution of λ introduced (Eq. 17). The cumulative number of infections
249 is shown in Figure 2b) and shows, on average, between 6 and 8 millions people have been infected
250 by SARS-CoV-2 in France, depending on whether super-spreaders effects are taken into account
251 via heavy tails in the distribution of λ . The uncertainty range is extremely large, according to the
252 error propagation given by the stochastic fluctuations of the parameters (see²⁷ for explanations). It
253 extends from few hundred thousands individuals up to 15 millions. The error range is larger when
254 super-spreaders are modelled. The average is however close to the value proposed by the authors
255 in⁶⁰, who estimate a prevalence of $\sim 6\%$ of COVID-19 in the French population. Another realistic
256 feature of the model is the presence of an asymmetric behavior of the right tail of daily infections
257 distributions (Figure 2c) that has also been observed in real COVID-19 published data⁶¹.

258 b. Italy

259 For Italy, the first suspect COVID-19 case goes back to December 22nd, 2019, a 41-year-old
260 woman who could only be tested positive for SARS-CoV-2 antibodies in April 2020⁶². As initial

261 condition we therefore set $I(t = 1) = 1$ and $t = 1$ corresponds to December 22nd, 2019. As
 262 for France we use $R_0 = 2.68_{2.47}^{2.86}$ leading to $\gamma = 0.37$ if fixing $\lambda_0 \simeq 1$. A first semi-lockdown
 263 was set in Italy on March 9th, 2020 ($t = 78$) and enforced on March 22nd, 2020 ($t = 89$). To
 264 simulate these two-steps lockdown we again base our reduction in R_0 on the mobility data for
 265 Italy which show for the first part of the confinement a reduction of about 50 % and a similar
 266 reduction to France (75%) for the strict lockdown phase. Figure 3 shows the results for the first
 267 wave. The initial condition on susceptible individuals is fixed to $S(1) = 6.0 \cdot 10^7$ corresponding
 268 to the estimate of the Italian population. A clear difference emerges with respect to the case of
 269 France in the behavior of R_0 which shows an intermediate reduction near $t = 80$, corresponding to
 270 March 11th, 2020, to $R_0 \simeq 1.4$ before reaching the final value of $R_0 \simeq 0.7$. This sort of "step" into
 271 the R_0 time behavior corresponds to the time interval between semi- and full-lockdown measures,
 272 whose efficiency significantly increases after March 24th, 2020, also corresponding to the peak
 273 value of infections. This is confirmed by looking at daily infections distributions (Figure 3c) that
 274 shows a peak value near March 24th, 2020, also observed in real COVID-19 data³⁰. Note that,
 275 as for France, the magnitude of the fluctuations depends on the presence of super-spreaders. The
 276 cumulative number of infections (Figure 3b) shows that, on average, almost 10 millions people
 277 have been infected by SARS-CoV-2 in Italy, ranging between few hundred thousands up to 15
 278 millions due to the the error propagation by the stochastic fluctuations of model parameters (see²⁷
 279 for explanations), with the range depending on the presence of super-spreaders. Nevertheless the
 280 wide range of uncertainty the average value is close to the value estimated from a team of experts of
 281 the Imperial College London according to which the 9.6% of Italian population has been infected,
 282 with a 95% confidence level ranging between 3.2% and 26%⁶³. These estimates correspond to
 283 cumulative infections of ~ 6 millions, ranging from ~ 2 and ~ 16 millions, well in agreement with
 284 our model and other statistical estimates⁶⁴.

285 **B. Future epidemics scenarios**

286 After lockdown measures are released, for both countries, we model three different scenarios:
 287 a first one where all restrictions are lifted (back to normality), a second one where strict distanc-
 288 ing measures are taken and a third one where the population remains mostly confined (partial
 289 lockdown).

290 *a. France*

291 Results for France are shown in Figure 4. From top to bottom panels we increase σ of the
292 log-normal distribution (Eq. 17) to model the presence of super-spreaders. Lockdown is released
293 at $t = 136$, corresponding to May 11th, 2020. The back to normality (red) scenario clearly shows
294 a second wave of infections peaking in summer (early July) and forcing group immunity in the
295 French population. The distancing measures (green) scenario, corresponding to a reduction of the
296 mobility of about 50%, leads to a second wave as intense as the first wave, but longer, at the end
297 of August. As in the previous scenario, the distancing measures scenario allows to reach a group
298 immunity in France. A third partial lockdown scenario is modelled (blue). This latter scenario sim-
299 ulates an $R_0 \simeq 1$, that can be achieved by imposing strict distancing measures, partial lockdowns
300 in cities with active clusters and contact tracking. It results in a linear modest increase of the total
301 number of infections that does not produce a proper wave of infections. As in the first wave mod-
302 elling, large uncertainties are also present in future scenarios although the three distinct behaviors
303 clearly appear. Finally, the presence of super spreaders may introduce an additional difficulties in
304 controlling partial lockdown scenarios. By comparing Figure 4b) and h) we observe that super-
305 spreaders can trigger an important growth of infections during positive fluctuations of R_0 although
306 its mean value is kept, by construction, constant. Another important effect of super-spreaders is
307 to increase the uncertainty on the infection counts: error bars for $\sigma = 0.6$ (Figure 4g,h,i) are two
308 times wider than those for $\sigma = 0.2$ (Figure 4a,b,c).

309 *b. Italy*

310 Figure 5 shows the results for modeling future epidemic scenarios for Italy. The first relaxation
311 of lockdown measures started at $t = 131$, corresponding to May 4th, 2020, while strict measures
312 were finally released at $t = 146$, corresponding to May 18th, 2020. The back to normality (red)
313 scenario moves towards a second wave of infections whose peak occurs at $t = 193$, correspond-
314 ing to July 4th, 2020, exactly three months after initial lockdown measures were released (May
315 4th, 2020). This would lead the so-called herd immunity for the whole Italian population (see Fig-
316 ure 5b), with a peak of daily infections near 5 millions of people (Figure 5c), and R_0 re-approaching
317 the initial value ($R_0 = 2.68$). The distancing measures (green) scenario produces a second wave
318 mostly similar, in terms of intensity, as the first wave, but occurring at $t = 246$, e.g., August 26th,
319 2020. This scenario will lead to 40 millions infected people, spanning between 25 and 55 millions,
320 thus producing a group immunity in Italy. A third scenario is modelled in which partial lockdown
321 measures are taken (blue). This latter scenario leads to a more controlled evolution of cumula-

322 tive infections which still remain practically unchanged with respect to the first wave cumulative
323 number. It has been obtained by simulating an $R_0 \simeq 1$, resulting from strict distancing measures
324 and reduced mobility, and does not produce a proper wave of infections. However, all scenarios
325 are clearly characterized by a wide range of uncertainties, although producing three well distinct
326 behaviors in both cumulative and daily infections. The same conclusions made for France apply
327 to Italy when it comes to the role of super-spreaders.

328 C. Phase Diagrams

329 In the previous section we have seen that increasing R_0 above 1 can or not produce a second
330 wave of infections and introduce also a time delay in the appearance of a second wave of infections.
331 We now analyse this effect in a complete phase diagram fashion. Phase diagrams are a standard
332 tool used in statistical physics to visualize allowed and forbidden states for selected variables of
333 complex systems and they have already been used in epidemiology⁶⁵. Phase diagrams will help us
334 to visualize for which values of R_0 we will observe a second wave of infections. Figures 6-7 show
335 the phase diagrams for France and for Italy, respectively. Panels a,b) show results for $\sigma = 0.2$,
336 c,d) for $\sigma = 0.4$ and e,f) for $\sigma = 0.6$. The diagrams are built in terms of ensemble averages of
337 number of infections per day $I(t)$ versus the average value of R_0 after the confinement (panels a),
338 and the errors (represented as standard deviation of the average $I(t)$ over the 30 realisations) are
339 shown in panels b. First we note that despite some small differences in the delay of the COVID-19
340 second wave of infections peak, the diagrams are very similar. In order to avoid a second wave,
341 R_0 could fluctuate on values even slightly larger than one only if super-spreaders are not included.
342 If super-spreaders are active, even small fluctuations of $R_0 > 1$ can trigger a second wave. Fur-
343 thermore, for $1.5 < R_0 < 2$, the second wave is delayed in Autumn or Winter 2020/2021 months.
344 The uncertainty follows the same behavior as the average and it peaks when the number of daily
345 infections is maximum. This means that the ability to control the outcome of the epidemics is sig-
346 nificantly reduced if R_0 is too high. The addition of super-spreaders also enhances the uncertainty
347 in the infection counts, inducing large fluctuations which might be difficult to control with partial
348 lockdown measures.

349 V. DISCUSSION

350 France and Italy have faced a long phase of lockdown with severe restrictions in mobility and
351 social contacts. They have managed to reduce the number of daily COVID-19 infections drasti-
352 cally and released almost simultaneously lockdown measures. This paper addresses the possible
353 future scenarios of COVID-19 infections in those countries by using one of the simplest possible
354 model capable to reproduce the first wave of infections and to take into account uncertainties,
355 namely a stochastic SEIR model with fluctuating parameters.

356

357 We have first verified that the model is capable to reproduce the behavior of the first wave
358 of infections and provide an estimate of COVID-19 prevalence that is coherent with a-posteriori
359 estimates of the prevalence of the virus. The introduction of stochasticity accounts for the large
360 uncertainties in both the initial conditions as well as the fluctuations in the basic reproduction
361 number R_0 originating from changes in virus characteristics, mobility or misapplication in con-
362 finement measures. 30 realisations of the model have been produced and they show very different
363 COVID-19 prevalence after the first wave. The range goes from thousands of infected to tens of
364 millions of infections in both countries. Average values are compatible with those found in other
365 studies^{60,63} whose aim was to estimate the prevalence of the virus. Nevertheless, we would like
366 to stress that the corresponding number of infected people that was detected in France and Italy
367 during the first wave was, according to the official released data, around 200 thousand people.
368 This discrepancy mostly comes from undetected cases, that can be a number many times bigger
369 than the detected cases. The lower bound provided by the error-bars of the realisations of the
370 stochastic SEIR models is therefore a limit for how many COVID-19 cases occurred in reality and
371 it is at least as big as the number of detected cases for that period, for which data are available,
372 plus the number of undetected cases, which can only be estimated.

373

374 Then, we have modelled future epidemics scenarios by choosing specific fluctuating behaviors
375 for R_0 and performing again 30 realisations of the stochastic SEIR model. Despite the very large
376 uncertainties, distinct scenarios clearly appear from the noise. In particular, they suggest that a
377 second wave can be avoided even with R_0 values slightly larger than one. This means that actual
378 distancing measures which include the use of surgical masks, the reduction in mobility and the
379 active contact tracking can be effective in avoiding a second peak of infections without the need

380 of imposing further strict lockdown measures. The analysis of phase diagrams show that there is
381 a sharp transition between observing or not a second wave of infections when the value of R_0 is
382 larger than 1 and that the exact value depends on the presence or not of super-spreaders. Moreover,
383 the models show that the higher R_0 , the lower the ability to control the number of infections in the
384 epidemics. Similarly, if super-spreaders are particularly active, the infection counts are difficult to
385 control and a second wave can be triggered more easily.

386 This model has also evident deficiencies in representing the COVID-19 infections. First of all,
387 the choice of the initial conditions is conditioned by our ignorance on the diffusion of the virus in
388 France and Italy in December 2019. Furthermore, we are unable to verify on an extensive dataset
389 the outcome of the first wave: on one side antibodies blood tests have still a lower reliability⁶⁶ and
390 on the other they have not been applied on an extensive number of individuals to get reliable esti-
391 mates. On top of the data-driven limitations, we have those introduced by the use of compartment
392 models, as there are geographic, social and age differences in the spread of the COVID-19 disease
393 in both countries²¹. Furthermore, we also assume that fluctuations on the parameters of the SEIR
394 model are Gaussian (for the incubation and recovery rate) or log-normal (for the infection rate),
395 in order to simulate heavy tailed distributions^{61,67} however the underling (skewed) distribution is
396 unknown. Another interesting research pathway is related to include the different psychological
397 perception on the need of distancing measures depending, e.g. from the media coverage of the
398 COVID-19 epidemics^{68,69}. We would like to remark however that, to overcome these limitations,
399 one would need to fit more complex models and introduce additional parameters which can, at the
400 present stage, barely be inferred by the data.

401

402 Our choice to stick to the stochastic SEIR model is indeed driven by few factors: i) despite its
403 simplicity our model allows for the possibility of modeling realistically the uncertainties with the
404 stochastic fluctuations instead of adding new parameters whose inference may affect the results;
405 ii) despite regional differences, national infections counts during the first wave have followed, for
406 both France and Italy, a sigmoid function that could be modeled with the mean field SEIR model
407 introduced in the present study. iii) unlike the UK or the US, both France and Italy have dealt with
408 the epidemics with a national centralized approach: whenever intensive care facilities were saturat-
409 ing in one region, patients' transfers have been operated to other national hospitals. iv) lockdown
410 measures have been applied uniformly on all the countries. v) introducing a spatial model also
411 introduces several additional parameters namely the interaction (exchange) coefficients among re-

412 gions (at least 20x20 coefficients for Italy and 13x13 coefficients for France). The deficiencies
413 of the COVID-19 testing capacities in many regions of both countries during the first phase pre-
414 vent from having a reasonable estimation of the parameters, introducing uncontrollable errors.
415 However, we acknowledge that, while the above mentioned factors were homogeneous across the
416 different regions of France and Italy, the evolution of the epidemic was very heterogeneous be-
417 tween different regions and even departments in Italy and France, with certain departments having
418 undergone saturation of the health care system (e.g. Lombardy and Bergamo in particular in Italy,
419 or Strasburg and the Grand-Est region in France), and others remaining almost untouched by the
420 epidemic. Moreover, geographical differences in Italy are present also in the measures after the
421 removal of the lockdown, with masks being compulsory only in certain areas. There are there-
422 fore also several good reasons to go beyond the presented mean field SEIR models whenever high
423 quality data will be available at a regional level.

424 This study can be applied to other countries, and this is why we publish the code of our analysis
425 alongside with the paper. To date, Northern Europe, UK, US and other American countries are
426 still facing the first wave of infections, so that future scenarios cannot be devised with the same
427 clarity as those outlined in this study for France and Italy. Other studies are currently focusing
428 on the second-wave modeling with different approaches. In⁷⁰⁻⁷², deterministic SIR models are
429 employed to forecast the second wave of COVID-19 infections for Washtenaw County, Iran and
430 France. These models are extended to include other variables which represent explicitly the num-
431 ber of patients taken to hospital or to intensive care units. However, their deterministic nature does
432 not allow for propagating the uncertainty in the variables and therefore to get an estimate of the
433 fluctuations in the number of hospitalized patients. In future studies, it could be interesting to add
434 the kind stochasticity suggested in the present study, to the extended SIR models proposed by⁷⁰⁻⁷²
435 in order to estimate range of uncertainties for hospitals and intensive care units.

436 VI. ACKNOWLEDGMENTS

437 DF acknowledges All the London Mathematical Laboratory fellows, B Dubrulle, F Pons, N
438 Bartolo, F Daviaud, P Yiou, M Kagayema, S Fromang and G Ramstein for useful discussions. TA
439 acknowledges G Consolini and M Materassi for useful discussions.

440 VII. DATA AVAILABILITY

441 The data that support the findings of this study are openly available in <https://systems.jhu.edu/research/public-health/ncov/>, maintained by Johns Hopkins University Center
442 for Systems Science. All figures scripts are available at <https://mycore.core-cloud.net/index.php/s/x8Wm4YyDVqEF2Xa>.
443
444

445 VIII. APPENDIX A: NUMERICAL CODE

```
446 % This appendix contains the MATLAB code used to perform
447 % the analysis contained in the paper via a stochastic
448 % SEIR model
449
450 %%VARIABLES INITIALIZATION
451 S=zeros(1,tmax);
452 E=zeros(1,tmax);
453 I=zeros(1,tmax);
454 R=zeros(1,tmax);
455 C=zeros(1,tmax);
456 %%PARAMETERS
457 %\lambda Infection Rate is equal to 1
458 lambda0=1;
459 % alpha is the inverse of the incubation period (1/t_incubation)
460 alpha0=0.27;
461 % R0 is equal to 2.68
462 R0=2.68;
463 % gamma is the inverse of the mean infectious period
464 gamma0=lambda0./R0;
465
466 % INITIAL CONDITIONS
467 S(1)=67000000;
468 I(1)=1;
```

```

469 R(1)=0;
470 T(1)=0;
471 C(1)=0;
472 gamma(1)=gamma0;
473 alpha(1)=alpha0;
474 lambda(1)=lambda0./S(1);
475
476 % EULER SCHEME FOR THE SDEs
477 for t=1:1:tmax./dt
478
479 R0(t+1)=lambda(t)./gamma0;
480 T(t+1)=t.*dt^2;
481 S(t+1)=S(t)-(lambda(t)*S(t)*I(t)).*dt;
482 E(t+1)=E(t)+((lambda(t)*S(t)*I(t))-alpha(t)*E(t)).*dt;
483 I(t+1)=I(t) +(alpha(t)*E(t) -gamma(t)*I(t)).*dt;
484 R(t+1)=R(t)+(gamma(t)*I(t)).*dt;
485 lambda(t+1)=(lambda0*dt+lambda0./5Ty*randn*sqrt(dt))./S(1);
486 gamma(t+1)=gamma0*dt+gamma0./5*randn*sqrt(dt);
487 alpha(t+1)=alpha0*dt+alpha0./5*randn*sqrt(dt);
488
489 %cumulative infected
490 C(t+1)=gamma0.*sum(I);
491
492 end
493

```

494 REFERENCES

495 ¹E. R. Gaunt, A. Hardie, E. C. Claas, P. Simmonds, and K. E. Templeton, “Epidemiology and
496 clinical presentations of the four human coronaviruses 229e, hku1, nl63, and oc43 detected
497 over 3 years using a novel multiplex real-time pcr method,” *Journal of clinical microbiology* **48**,
498 2940–2947 (2010).

499 ²J. Wu, W. Cai, D. Watkins, and J. Glanz, “How the virus got out,” *The New York Times* (2020).

500 ³W. H. Organization *et al.*, “Coronavirus disease 2019 (covid-19): situation report, 51,” (2020).

501 ⁴C. COVID and R. Team, “Severe outcomes among patients with coronavirus disease 2019
502 (covid-19)—united states, february 12–march 16, 2020,” *MMWR Morb Mortal Wkly Rep* **69**,
503 343–346 (2020).

504 ⁵Y.-Y. Zheng, Y.-T. Ma, J.-Y. Zhang, and X. Xie, “Covid-19 and the cardiovascular system,”
505 *Nature Reviews Cardiology* **17**, 259–260 (2020).

506 ⁶C. Huang, Y. Wang, X. Li, L. Ren, J. Zhao, Y. Hu, L. Zhang, G. Fan, J. Xu, X. Gu, *et al.*,
507 “Clinical features of patients infected with 2019 novel coronavirus in wuhan, china,” *The Lancet*
508 **395**, 497–506 (2020).

509 ⁷M. Cascella, M. Rajnik, A. Cuomo, S. C. Dulebohn, and R. Di Napoli, “Features, evaluation
510 and treatment coronavirus (covid-19),” in *Statpearls [internet]* (StatPearls Publishing, 2020).

511 ⁸R. M. Anderson, H. Heesterbeek, D. Klinkenberg, and T. D. Hollingsworth, “How will country-
512 based mitigation measures influence the course of the covid-19 epidemic?” *The Lancet* **395**,
513 931–934 (2020).

514 ⁹M. Chinazzi, J. T. Davis, M. Ajelli, C. Gioannini, M. Litvinova, S. Merler, A. Pas-
515 tore y Piontti, K. Mu, L. Rossi, K. Sun, C. Viboud, X. Xiong, H. Yu, M. E. Hal-
516 loran, I. M. Longini, and A. Vespignani, “The effect of travel restrictions on the
517 spread of the 2019 novel coronavirus (covid-19) outbreak,” *Science* **368**, 395–400 (2020),
518 <https://science.sciencemag.org/content/368/6489/395.full.pdf>.

519 ¹⁰H.-Y. Yuan, G. Han, H. Yuan, S. Pfeiffer, A. Mao, L. Wu, and D. Pfeiffer, “The importance
520 of the timing of quarantine measures before symptom onset to prevent covid-19 outbreaks - il-
521 lustrated by hong kong’s intervention model,” *medRxiv* (2020), 10.1101/2020.05.03.20089482,
522 <https://www.medrxiv.org/content/early/2020/05/06/2020.05.03.20089482.full.pdf>.

523 ¹¹R. H. Mena, J. X. Velasco-Hernandez, N. B. Mantilla-Beniens, G. A. Carranco-Sapiéns,
524 L. Benet, D. Boyer, and I. P. Castillo, “Using the posterior predictive distribution to analyse
525 epidemic models: Covid-19 in mexico city,” *arXiv preprint arXiv:2005.02294* (2020).

526 ¹²S. Khajanchi and K. Sarkar, “Forecasting the daily and cumulative number of cases for the covid-
527 19 pandemic in india,” *Chaos: An Interdisciplinary Journal of Nonlinear Science* **30**, 071101
528 (2020).

529 ¹³K. Sarkar, S. Khajanchi, and J. J. Nieto, “Modeling and forecasting the covid-19 pandemic in
530 india,” *Chaos, Solitons & Fractals* **139**, 110049 (2020).

- 531 ¹⁴N. Fernandes, “Economic effects of coronavirus outbreak (covid-19) on the world economy,”
532 Available at SSRN 3557504 (2020).
- 533 ¹⁵O. Coibion, Y. Gorodnichenko, and M. Weber, “Labor markets during the covid-19 crisis: A
534 preliminary view,” Tech. Rep. (National Bureau of Economic Research, 2020).
- 535 ¹⁶N. Cellini, N. Canale, G. Mioni, and S. Costa, “Changes in sleep pattern, sense of time and
536 digital media use during covid-19 lockdown in italy,” *Journal of Sleep Research*, e13074 (2020).
- 537 ¹⁷H. A. Rothan and S. N. Byrareddy, “The epidemiology and pathogenesis of coronavirus disease
538 (covid-19) outbreak,” *Journal of autoimmunity*, 102433 (2020).
- 539 ¹⁸N. Chintalapudi, G. Battineni, and F. Amenta, “Covid-19 disease outbreak forecasting of reg-
540 istered and recovered cases after sixty day lockdown in italy: A data driven model approach,”
541 *Journal of Microbiology, Immunology and Infection* (2020).
- 542 ¹⁹M. Gatto, E. Bertuzzo, L. Mari, S. Miccoli, L. Carraro, R. Casagrandi, and A. Rinaldo,
543 “Spread and dynamics of the covid-19 epidemic in italy: Effects of emergency contain-
544 ment measures,” *Proceedings of the National Academy of Sciences* **117**, 10484–10491 (2020),
545 <https://www.pnas.org/content/117/19/10484.full.pdf>.
- 546 ²⁰J. Roux, C. Massonnaud, and P. Crépey, “Covid-19: One-month impact of the french lockdown
547 on the epidemic burden,” *medRxiv* (2020).
- 548 ²¹L. Di Domenico, G. Pullano, C. E. Sabbatini, P.-Y. Boëlle, and V. Colizza, “Expected impact of
549 lockdown in île-de-france and possible exit strategies,” *medRxiv* (2020).
- 550 ²²B. Ghoshal and A. Tucker, “Estimating uncertainty and interpretability in deep learning for
551 coronavirus (covid-19) detection,” *arXiv preprint arXiv:2003.10769* (2020).
- 552 ²³T. Hale, A. Petherick, T. Phillips, and S. Webster, “Variation in government responses to covid-
553 19,” *Blavatnik School of Government Working Paper* **31** (2020).
- 554 ²⁴R. Li, S. Pei, B. Chen, Y. Song, T. Zhang, W. Yang, and J. Shaman, “Substantial undocumented
555 infection facilitates the rapid dissemination of novel coronavirus (sars-cov2),” *Science* (2020).
- 556 ²⁵R. Nunes-Vaz, “Visualising the doubling time of covid-19 allows comparison of the success of
557 containment measures,” *Global Biosecurity* **1** (2020).
- 558 ²⁶A. N. Desai, M. U. Kraemer, S. Bhatia, A. Cori, P. Nouvellet, M. Herringer, E. L. Cohn, M. Car-
559 rion, J. S. Brownstein, L. C. Madoff, *et al.*, “Real-time epidemic forecasting: Challenges and
560 opportunities,” *Health security* **17**, 268–275 (2019).
- 561 ²⁷D. Faranda, I. P. Castillo, O. Hulme, A. Jezequel, J. S. W. Lamb, Y. Sato, and E. L. Thomp-
562 son, “Asymptotic estimates of sars-cov-2 infection counts and their sensitivity to stochastic

563 perturbation,” *Chaos: An Interdisciplinary Journal of Nonlinear Science* **30**, 051107 (2020),
564 <https://doi.org/10.1063/5.0008834>.

565 ²⁸J. O. Lloyd-Smith, S. J. Schreiber, P. E. Kopp, and W. M. Getz, “Superspreading and the effect
566 of individual variation on disease emergence,” *Nature* **438**, 355–359 (2005).

567 ²⁹F. Brauer, “Compartmental models in epidemiology,” in *Mathematical epidemiology* (Springer,
568 2008) pp. 19–79.

569 ³⁰T. Alberti and D. Faranda, “On the uncertainty of real-time predictions of epidemic growths: A
570 covid-19 case study for china and italy,” *Communications in Nonlinear Science and Numerical*
571 *Simulation* **90**, 105372 (2020).

572 ³¹G. Consolini and M. Materassi, “A stretched logistic equation for pandemic spreading,” *Chaos,*
573 *Solitons Fractals* **140**, 110113 (2020).

574 ³²F. D’Emilio and N. Winfield, “Italy blasts virus panic as it eyes new testing criteria,” *abc News*
575 (2020).

576 ³³K. Arin, “Drive-thru clinics, drones: Korea’s new weapons in virus fight,” *The Korea Herald*
577 (2020).

578 ³⁴P. P. AGI, “Come vanno letti i dati sul coronavirus in italia,” *AGI Agenzia Italia* (2020).

579 ³⁵L. Ferrari, G. Gerardi, G. Manzi, A. Micheletti, F. Nicolussi, and S. Salini, “Modelling provin-
580 cial covid-19 epidemic data in italy using an adjusted time-dependent sird model,” (2020),
581 [arXiv:2005.12170 \[stat.AP\]](https://arxiv.org/abs/2005.12170).

582 ³⁶J. Cohen and K. Kupferschmidt, “Countries test tactics in ‘war’ against covid-19,” (2020).

583 ³⁷J. H. Tanne, E. Hayasaki, M. Zastrow, P. Pulla, P. Smith, and A. G. Rada, “Covid-19: how
584 doctors and healthcare systems are tackling coronavirus worldwide,” *Bmj* **368** (2020).

585 ³⁸P. Kellam and W. Barclay, “The dynamics of humoral immune responses following sars-cov-2
586 infection and the potential for reinfection,” *Journal of General Virology* , jgv001439 (2020).

587 ³⁹A. T. Xiao, C. Gao, and S. Zhang, “Profile of specific antibodies to sars-cov-2: the first report,”
588 *The Journal of infection* (2020).

589 ⁴⁰A. Grifoni, D. Weiskopf, S. I. Ramirez, J. Mateus, J. M. Dan, C. R. Moderbacher, S. A. Rawl-
590 ings, A. Sutherland, L. Premkumar, R. S. Jadi, *et al.*, “Targets of t cell responses to sars-cov-2
591 coronavirus in humans with covid-19 disease and unexposed individuals,” *Cell* (2020).

592 ⁴¹L. Ni, F. Ye, M.-L. Cheng, Y. Feng, Y.-Q. Deng, H. Zhao, P. Wei, J. Ge, M. Gou, X. Li, *et al.*,
593 “Detection of sars-cov-2-specific humoral and cellular immunity in covid-19 convalescent indi-
594 viduals,” *Immunity* (2020).

- 595 ⁴²S. M. Kissler, C. Tedijanto, E. Goldstein, Y. H. Grad, and M. Lipsitch, “Projecting the transmis-
596 sion dynamics of sars-cov-2 through the postpandemic period,” *Science* **368**, 860–868 (2020).
- 597 ⁴³J. T. Wu, K. Leung, and G. M. Leung, “Nowcasting and forecasting the potential domestic and
598 international spread of the 2019-ncov outbreak originating in wuhan, china: a modelling study,”
599 *The Lancet* **395**, 689–697 (2020).
- 600 ⁴⁴L. Peng, W. Yang, D. Zhang, C. Zhuge, and L. Hong, “Epidemic analysis of covid-19 in china
601 by dynamical modeling,” arXiv preprint arXiv:2002.06563 (2020).
- 602 ⁴⁵S. A. Lauer, K. H. Grantz, Q. Bi, F. K. Jones, Q. Zheng, H. R. Meredith, A. S. Azman, N. G.
603 Reich, and J. Lessler, “The incubation period of coronavirus disease 2019 (covid-19) from
604 publicly reported confirmed cases: Estimation and application,” *Annals of Internal Medicine*
605 (2020).
- 606 ⁴⁶E. Lavezzo, E. Franchin, C. Ciavarella, G. Cuomo-Dannenburg, L. Barzon, C. Del Vec-
607 chio, L. Rossi, R. Manganelli, A. Loregian, N. Navarin, D. Abate, M. Sciro, S. Merigliano,
608 E. Decanale, M. C. Vanuzzo, F. Saluzzo, F. Onelia, M. Pacenti, S. Parisi, G. Car-
609 retta, D. Donato, L. Flor, S. Cocchio, G. Masi, A. Sperduti, L. Cattarino, R. Sal-
610 vador, K. A. Gaythorpe, , A. R. Brazzale, S. Toppo, M. Trevisan, V. Baldo, C. A.
611 Donnelly, N. M. Ferguson, I. Dorigatti, and A. Crisanti, “Suppression of covid-19 out-
612 break in the municipality of vo, italy,” medRxiv (2020), 10.1101/2020.04.17.20053157,
613 <https://www.medrxiv.org/content/early/2020/04/18/2020.04.17.20053157.full.pdf>.
- 614 ⁴⁷L. F. Olsen and W. M. Schaffer, “Chaos versus noisy periodicity: alternative hypotheses for
615 childhood epidemics,” *Science* **249**, 499–504 (1990).
- 616 ⁴⁸H. Andersson and T. Britton, *Stochastic epidemic models and their statistical analysis*, Vol. 151
617 (Springer Science & Business Media, 2012).
- 618 ⁴⁹J. Dureau, K. Kalogeropoulos, and M. Baguelin, “Capturing the time-varying drivers of an
619 epidemic using stochastic dynamical systems,” *Biostatistics* **14**, 541–555 (2013).
- 620 ⁵⁰J. A. Polonsky, A. Baidjoe, Z. N. Kamvar, A. Cori, K. Durski, W. J. Edmunds, R. M. Eggo,
621 S. Funk, L. Kaiser, P. Keating, *et al.*, “Outbreak analytics: a developing data science for in-
622 forming the response to emerging pathogens,” *Philosophical Transactions of the Royal Society*
623 **B 374**, 20180276 (2019).
- 624 ⁵¹G. Viceconte and N. Petrosillo, “Covid-19 r0: Magic number or conundrum?” *Infectious Disease*
625 *Reports* **12** (2020).
- 626 ⁵²I. Kashnitsky, “Covid-19 in unequally ageing european regions,” (2020).

627 ⁵³D. Faranda and S. Vaienti, “Extreme value laws for dynamical systems under observational
628 noise,” *Physica D: Nonlinear Phenomena* **280**, 86–94 (2014).

629 ⁵⁴D. Faranda, Y. Sato, B. Saint-Michel, C. Wiertel, V. Padilla, B. Dubrulle, and F. Daviaud,
630 “Stochastic chaos in a turbulent swirling flow,” *Physical review letters* **119**, 014502 (2017).

631 ⁵⁵J. Zhang, M. Litvinova, W. Wang, Y. Wang, X. Deng, X. Chen, M. Li, W. Zheng, L. Yi, X. Chen,
632 *et al.*, “Evolving epidemiology and transmission dynamics of coronavirus disease 2019 out-
633 side hubei province, china: a descriptive and modelling study,” *The Lancet Infectious Diseases*
634 (2020).

635 ⁵⁶J. A. Al-Tawfiq and A. J. Rodriguez-Morales, “Super-spreading events and contribution to trans-
636 mission of mers, sars, and covid-19,” (2020).

637 ⁵⁷A. Deslandes, V. Berti, Y. Tandjaoui-Lambotte, C. Alloui, E. Carbonnelle, J. Zahar, S. Briclher,
638 and Y. Cohen, “Sars-cov-2 was already spreading in france in late december 2019,” *International*
639 *Journal of Antimicrobial Agents* , 106006 (2020).

640 ⁵⁸G. Pullano, E. Valdano, N. Scarpa, S. Rubrichi, and V. Colizza, “Population mobility reductions
641 during covid-19 epidemic in france under lockdown,” .

642 ⁵⁹H. Salje, C. T. Kiem, N. Lefrancq, N. Courtejoie, P. Bosetti, J. Paireau, A. Andronico, N. Hoze,
643 J. Richet, C.-L. Dubost, *et al.*, “Estimating the burden of sars-cov-2 in france,” *Science* (2020).

644 ⁶⁰H. Salje, C. Tran Kiem, N. Lefrancq, N. Courtejoie, P. Bosetti, J. Paireau, A. An-
645 dronico, N. Hozé, J. Richet, C.-L. Dubost, Y. Le Strat, J. Lessler, D. Levy-
646 Bruhl, A. Fontanet, L. Opatowski, P.-Y. Boelle, and S. Cauchemez, “Estimat-
647 ing the burden of sars-cov-2 in france,” *Science* (2020), 10.1126/science.abc3517,
648 <https://science.sciencemag.org/content/early/2020/05/12/science.abc3517.full.pdf>.

649 ⁶¹M. Maleki, M. R. Mahmoudi, D. Wraith, and K.-H. Pho, “Time series modelling to forecast the
650 confirmed and recovered cases of covid-19,” *Travel Medicine and Infectious Disease* , 101742
651 (2020).

652 ⁶²“Coronavirus milano, la 41enne con la febbre il 22 dicembre: «ora hanno trovato gli anticorpi al
653 covid»,” *Corriere della Sera* (2020).

654 ⁶³S. Flaxman, S. Mishra, A. Gandy, H. Unwin, H. Coupland, T. Mellan, H. Zhu, T. Berah, J. Eaton,
655 P. Perez Guzman, *et al.*, “Report 13: Estimating the number osars-cov-2figf infections and the
656 impact of non-pharmaceutical interventions on covid-19 in 11 european countries,” (2020).

657 ⁶⁴G. De Natale, V. Ricciardi, G. De Luca, D. De Natale, G. Di Meglio, A. Fer-
658 ragamo, V. Marchitelli, A. Piccolo, A. Scala, R. Somma, E. Spina, and

659 C. Troise, “The covid-19 infection in italy: a statistical study of an ab-
660 normally severe disease,” medRxiv (2020), 10.1101/2020.03.28.20046243,
661 <https://www.medrxiv.org/content/early/2020/04/10/2020.03.28.20046243.full.pdf>.

662 ⁶⁵L. Wang and X. Li, “Spatial epidemiology of networked metapopulation: An overview,” Chinese
663 Science Bulletin **59**, 3511–3522 (2014).

664 ⁶⁶Q.-X. Long, B.-Z. Liu, H.-J. Deng, G.-C. Wu, K. Deng, Y.-K. Chen, P. Liao, J.-F. Qiu, Y. Lin,
665 X.-F. Cai, *et al.*, “Antibody responses to sars-cov-2 in patients with covid-19,” Nature Medicine
666 , 1–4 (2020).

667 ⁶⁷Y. Liu, R. M. Eggo, and A. J. Kucharski, “Secondary attack rate and superspreading events for
668 sars-cov-2,” The Lancet **395**, e47 (2020).

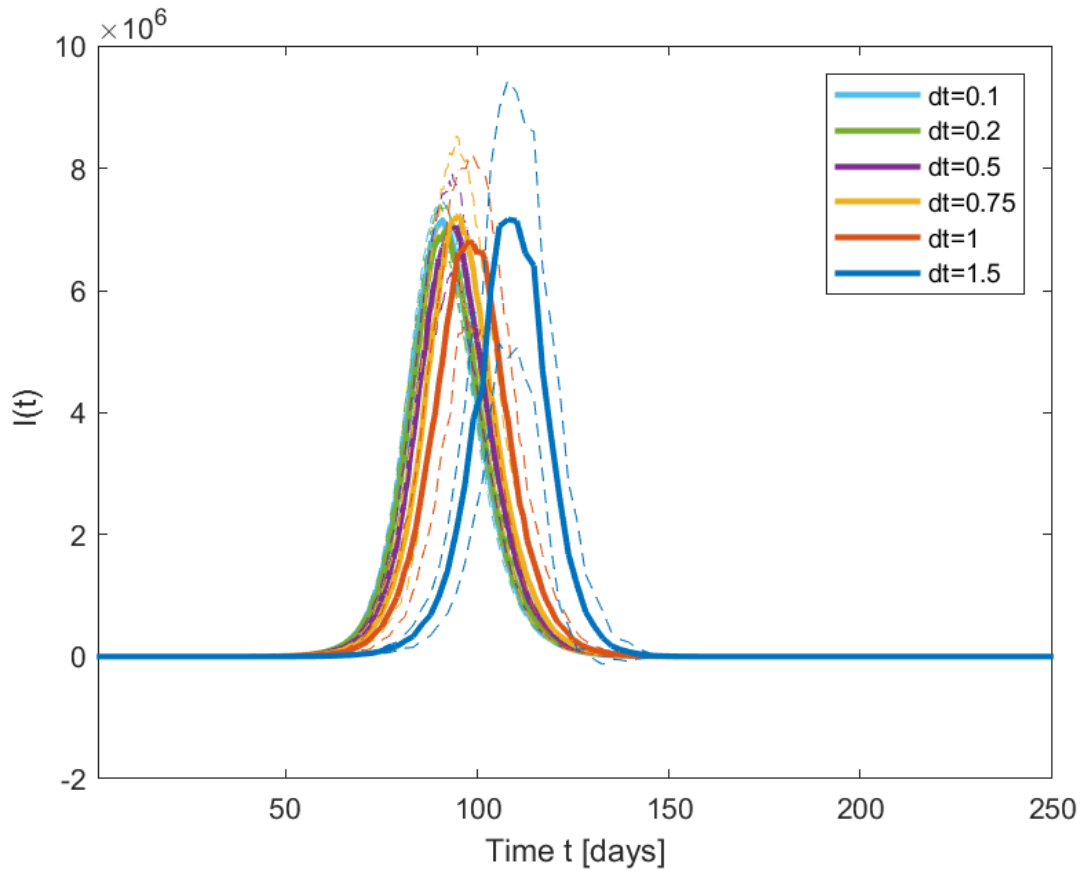
669 ⁶⁸A. d’Onofrio, P. Manfredi, and E. Salinelli, “Vaccinating behaviour, information, and the dy-
670 namics of sir vaccine preventable diseases,” Theoretical population biology **71**, 301–317 (2007).

671 ⁶⁹S. Khajanchi, K. Sarkar, J. Mondal, and M. Perc, “Dynamics of the covid-19 pandemic in india,”
672 arXiv preprint arXiv:2005.06286 (2020).

673 ⁷⁰M. Renardy, M. Eisenberg, and D. Kirschner, “Predicting the second wave of covid-19 in washt-
674 enaw county, mi,” Journal of theoretical biology **507**, 110461 (2020).

675 ⁷¹B. Ghanbari, “On forecasting the spread of the covid-19 in iran: The second wave,” Chaos,
676 Solitons & Fractals **140**, 110176 (2020).

677 ⁷²J. Daunizeau, R. Moran, J. Brochard, J. Mattout, R. Frackowiak, and K. Friston, “Modelling
678 lockdown-induced secondary covid waves in france,” medRxiv (2020).



679

680 FIG. 1. Test of stability for the Susceptible-Exposed-Infected-Recovered (SEIR) model of COVID-19 for
 681 France (Eqs 10-16) with $\lambda = 1./S(0)$, $\alpha = 0.27$, $\gamma = 0.37$. Initial conditions are set to $I(1) = 1$, $S(1) =$
 682 $6.7 \cdot 10^7$ (French Population), $E(1) = R(1) = 0$. The SEIR model is integrated with different $0.1 < dt < 1.5$.
 683 Solid lines show the average for 30 realisations of the SEIR stochastic models, dotted lines extend to one
 684 standard deviation of the mean.

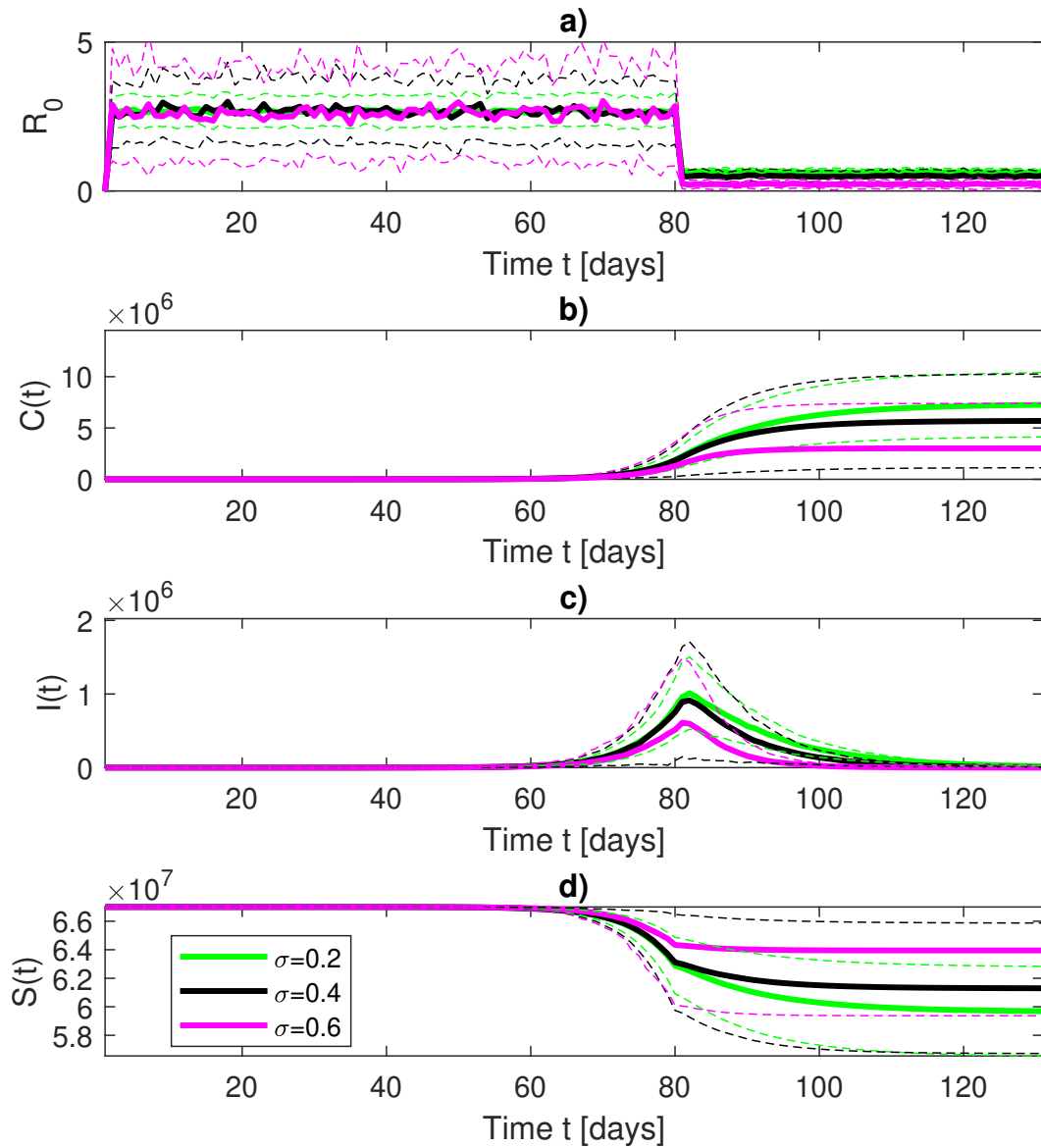


FIG. 2. Susceptible-Exposed-Infected-Recovered (SEIR) model of COVID-19 for France (Eqs 10-16) with $\lambda = 1./S(0)$, $\alpha = 0.27$, $\gamma = 0.37$, $dt = 1$. Initial conditions are set to $I(1) = 1$, $S(1) = 6.7 \cdot 10^7$, $E(1) = R(1) = 0$. $t = 1$ corresponds to Dec 27, 2019. Confinement is introduced at $t = 78$ (Mar 17, 2020). Time evolution for a) the basic reproduction number R_0 , (b) the cumulative number of infections $C(t)$, (c) the daily infected individuals $I(t)$, (d) the number of susceptible individuals $S(t)$. Solid lines show the average for 30 realisations of the SEIR stochastic models, shadings extend to one standard deviation of the mean. Colors represent different values of σ in the lognormal distribution of λ (Eq. 17 from light to heavy tails).

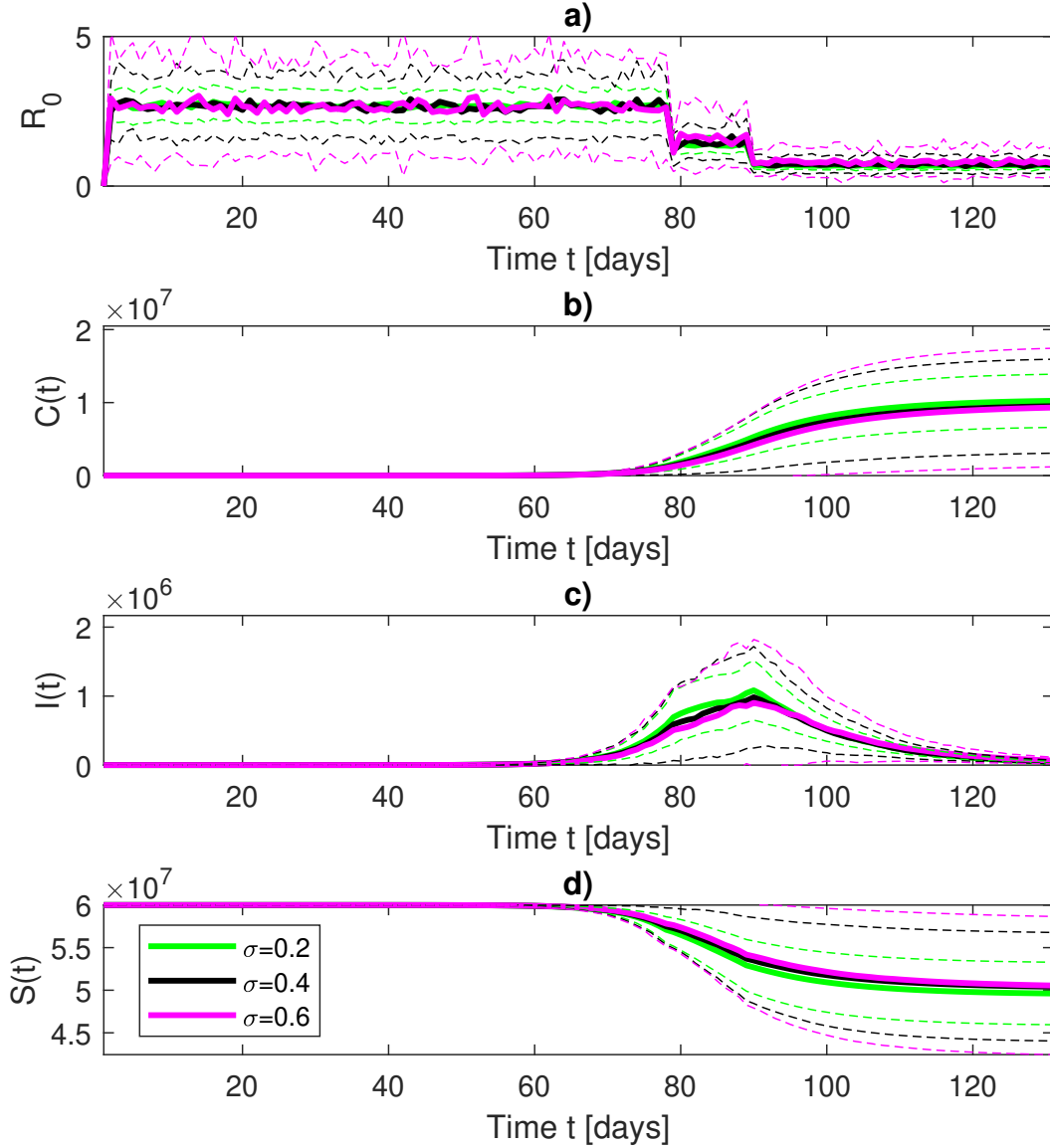


FIG. 3. Susceptible-Exposed-Infected-Recovered (SEIR) model of COVID-19 for Italy (Eqs 10-16) with $\lambda = 1./S(0)$, $\alpha = 0.27$, $\gamma = 0.37$, $dt = 1$. Initial conditions are set to $I(1) = 1$, $S(1) = 6.0 \cdot 10^7$, $E(1) = R(1) = 0$. $t = 1$ corresponds to Dec 22, 2019. First confinement measures are introduced at $t = 80$ (Mar 9, 2020) and enforced at $t = 89$ (Mar 22, 2020). Time evolution for a) the basic reproduction number R_0 , (b) the cumulative number of infections $C(t)$, (c) the daily infected individuals $I(t)$, (d) the number of susceptible individuals $S(t)$. Solid lines show the average for 30 realisations of the SEIR stochastic models, shadings extend to one standard deviation of the mean. Colors represent different values of σ in the lognormal distribution of λ (Eq. 17 from light to heavy tails).

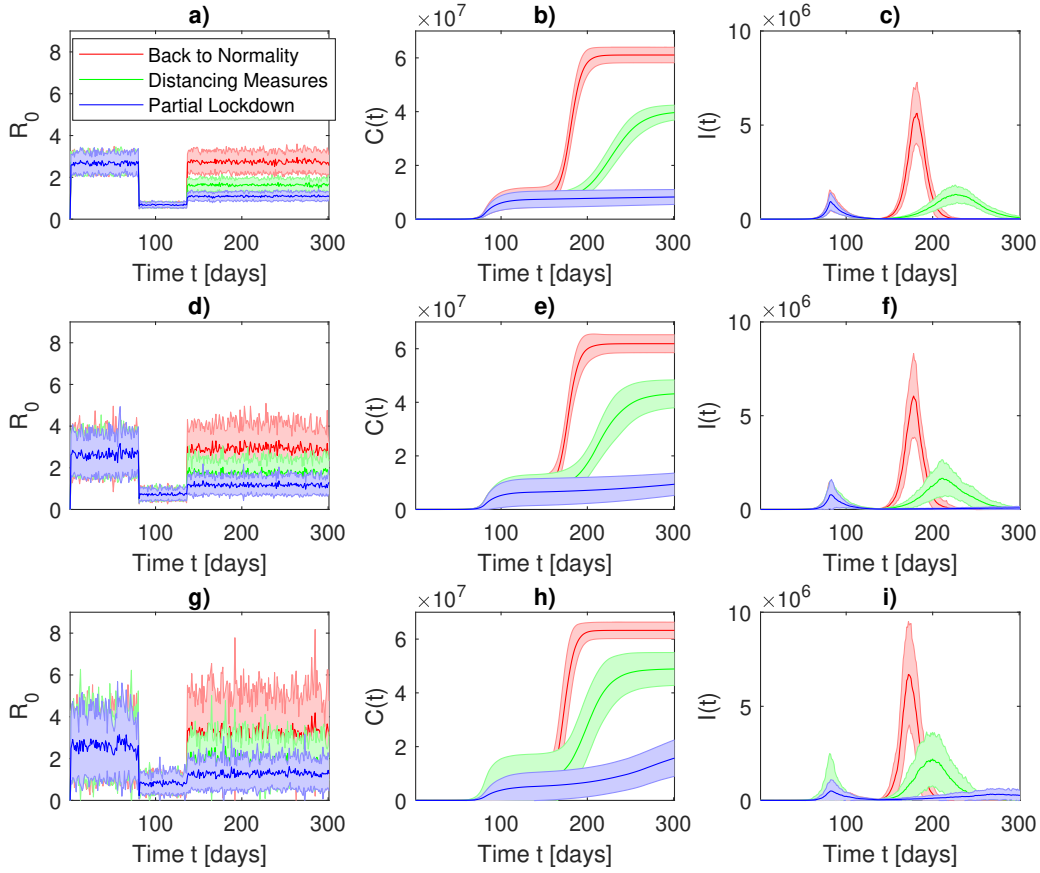


FIG. 4. Susceptible-Exposed-Infected-Recovered (SEIR) model of COVID-19 for the second wave in France. Initial conditions are set as in Figure 2. After the confinement is released ($t = 136$, May 11, 2020) three scenarios are modelled: back to normality (red), distancing measures (green), partial lockdown (blue). a,d,g) Time evolution for the basic reproduction number R_0 , b,e,h) Time evolution for the cumulative number of infections $C(t)$, c,f,i) Time evolution for the daily infected individuals $I(t)$. a,b,c) $\sigma = 0.2$ in, d,e,f) $\sigma = 0.4$, g,h,i) $\sigma = 0.6$ in the lognormal distribution for λ (Eq. 17). Solid lines show the average for 30 realisations of the SEIR stochastic models, shadings extend to one standard deviations of the mean.

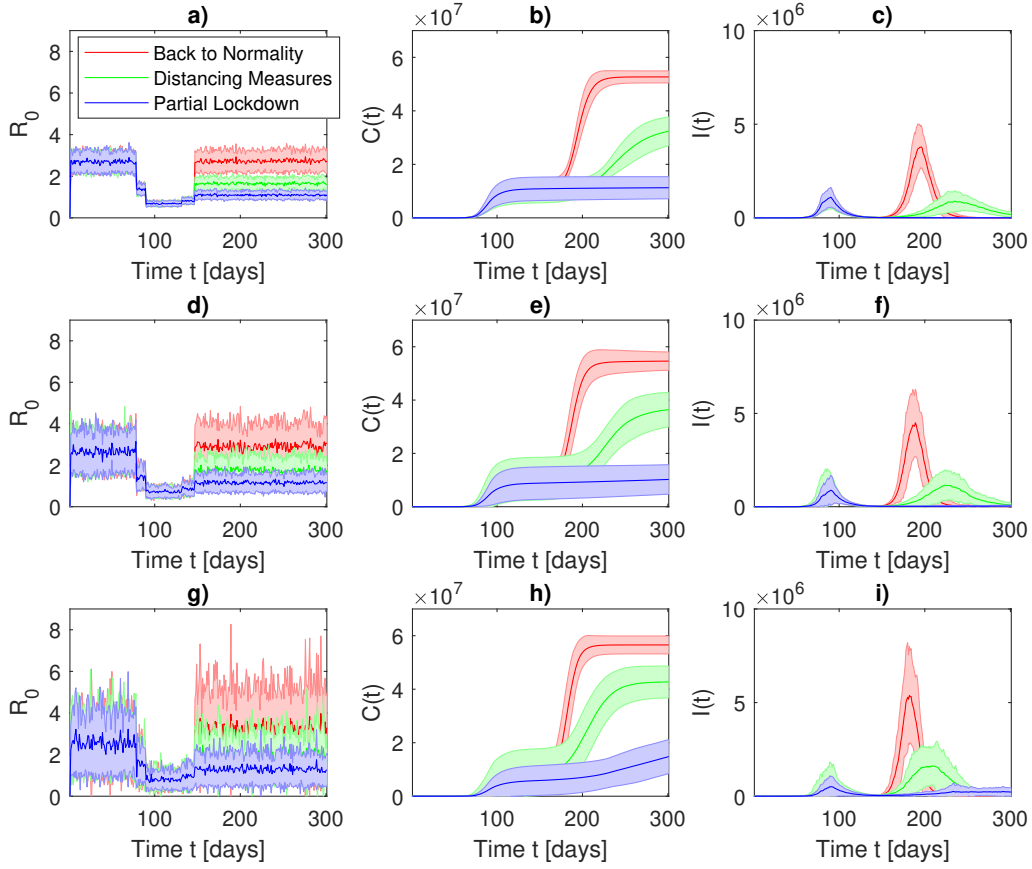


FIG. 5. Susceptible-Exposed-Infected-Recovered (SEIR) model of COVID-19 for the second wave in Italy. Initial conditions are set as in Figure 3. After the confinement is released ($t = 131$, May 4, 2020 and $t = 146$, May 18, 2020) three scenarios are modelled: back to normality (red), distancing measures (green), partial lockdown (blue). a,d,g) Time evolution for the basic reproduction number R_0 , b,e,h) Time evolution for the cumulative number of infections $C(t)$, c,f,i) Time evolution for the daily infected individuals $I(t)$. a,b,c) $\sigma = 0.2$ in, d,e,f) $\sigma = 0.4$, g,h,i) $\sigma = 0.6$ in the lognormal distribution for λ (Eq. 17). Solid lines show the average for 30 realisations of the SEIR stochastic models, shadings extend to one standard deviations of the mean.

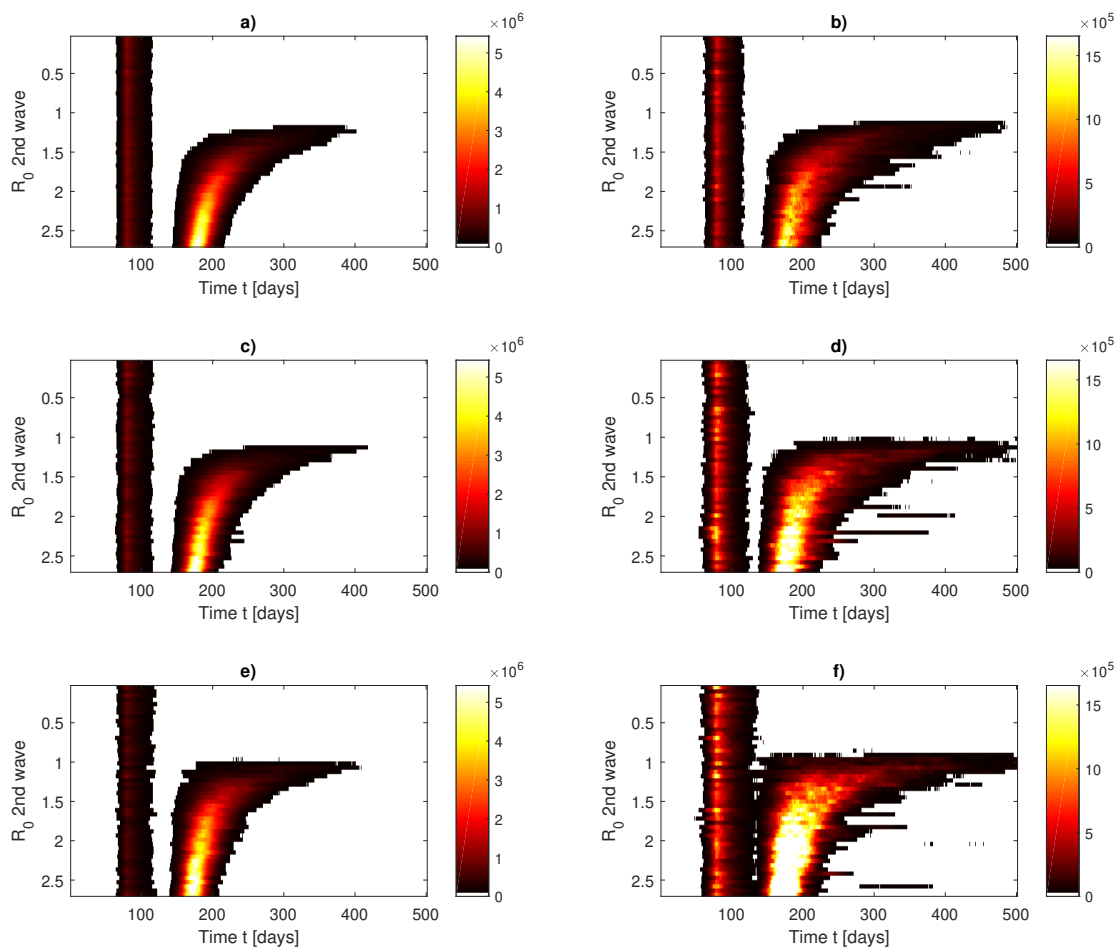


FIG. 6. Phase diagram for the Susceptible-Exposed-Infected-Recovered (SEIR) model of COVID-19 for the second wave in France. Initial conditions are set as in Figure 2. After the confinement is released ($t = 136$, May 11, 2020) all possible R_0 are modelled. a,c,e) Average of daily infected individuals $I(t)$. b,d,f) Standard deviation of daily infected individuals. Diagrams are obtained using 30 realisations of the SEIR models. a,b) $\sigma = 0.2$ in, c,d) $\sigma = 0.4$, e,f) $\sigma = 0.6$ in the lognormal distribution for λ (Eq. 17).

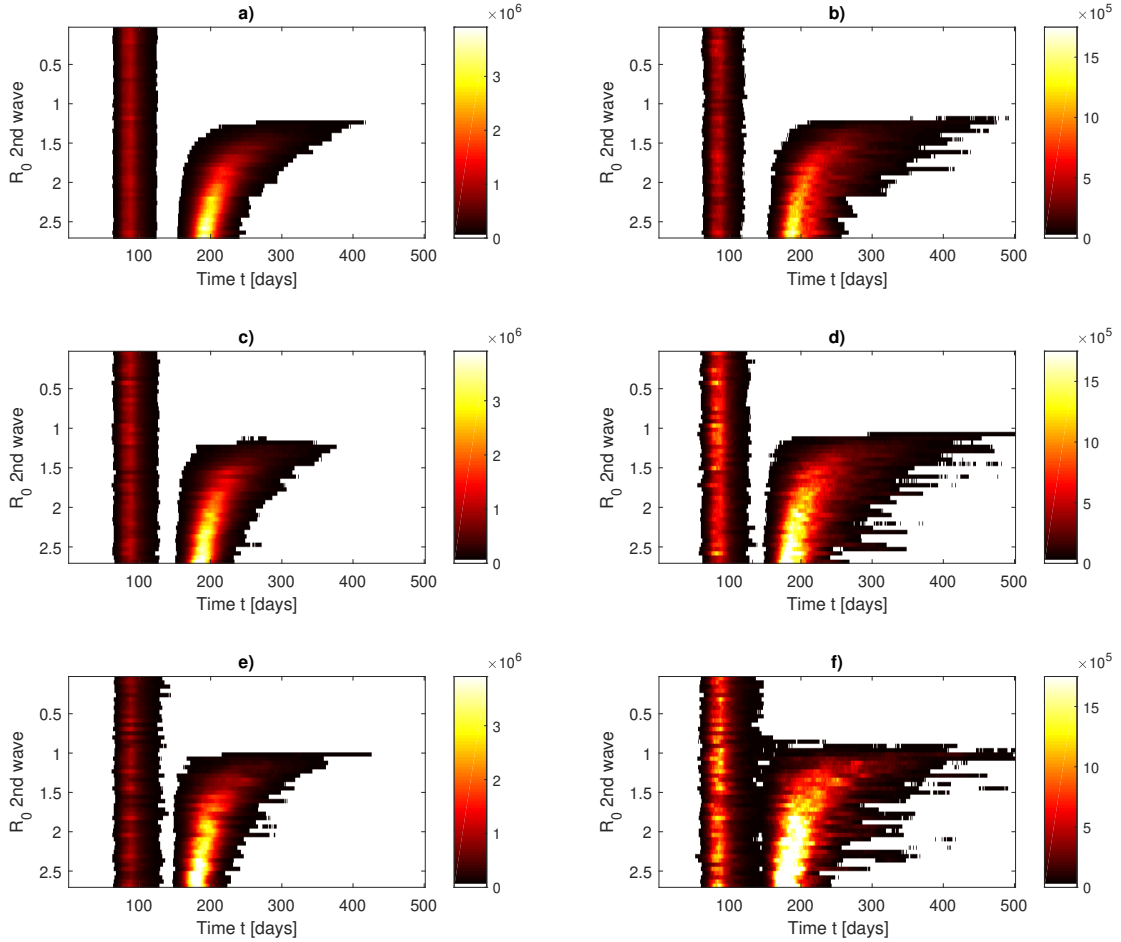


FIG. 7. Phase diagram for the Susceptible-Exposed-Infected-Recovered (SEIR) model of COVID-19 for the second wave in Italy. Initial conditions are set as in Figure 3. After the confinement is released ($t = 131$, May 4, 2020 and then $t = 146$ May 18, 2020) all possible R_0 are modelled. a,c,e) Average of daily infected individuals $I(t)$. b,d,f) Standard deviation of daily infected individuals. Diagrams are obtained using 30 realisations of the SEIR models. a,b) $\sigma = 0.2$ in, c,d) $\sigma = 0.4$, e,f) $\sigma = 0.6$ in the lognormal distribution for λ (Eq. 17).